Thermal-Induced Vaporization of Organic Materials

Mark P. Hoffman*
Science Applications International Corporation, Colorado Springs, Colorado 80906
and
Fred A. Rigby†
Science Applications International Corporation, Albuquerque, New Mexico 87106

A model for the rapid vaporization into a vacuum of graphite and graphitized char is presented. The model examines the effect on the carbon vaporization rate due to pyrolytic gases released from the decomposition of organic resins. The carbon mass flux is computed from the consideration of the gas kinetics of multiple noninteracting carbon species and a single pyrolytic gas species. A simplified approximation is presented that gives the carbon mass flux if the vaporizing surface temperature and the pyrolytic gas flux are known.

Introduction

AN understanding of the effects of energy radiation on organic composite structural materials is needed to assess the performance of these materials. High-energy radiation on organic composite materials results in thermochemical decomposition of the organic component. A mixture of gases is given off during the pyrolysis of the organic material, leaving behind a graphitic char. As the radiation heats the target, the surface can become sufficiently hot to vaporize the graphite while pyrolysis occurs below the surface. This paper presents a simple model of the gasdynamics for estimating the carbon mass flux for vaporizing graphite in the presence of a pyrolytic gas flux. The problem is treated as one dimensional in the direction normal to the vaporizing surface. Steady-state conditions are assumed to exist in the sense that the time scale of the gasdynamics that determines the mass flow rate is short compared to the rate of temperature change. The model assumes negligible heating of the gas by the heat source. (It would be necessary to modify the model by incorporating a gas heating term in order to account for energy absorption by the gas.) Although the model can be extended to include ablation of materials into an ambient atmosphere, the discussion in this paper concentrates on ablation into a vacuum.

Models for the rapid vaporization of single molecular species have been presented by Anisimov[1] and Knight.[2] Graphite, when it vaporizes, can form several different molecular species, and thus requires a more complex model that addresses each species. Baker[3] and Risch and Kelly[4] have addressed this problem. The presence of additional gas species emanating from the surface that, unlike carbon molecules, cannot recondense on the hot carbon surface requires an additional development of the vaporization model.

Under conditions of rapid vaporization the flux of molecules away from an ablating surface exceeds the backscattered flux returning to the surface. Within a few molecular mean free paths of the surface, the distribution of molecular velocities in the gas achieves translational equilibrium. A thin, nonequilibrium gas layer called the Knudsen layer develops near the surface. Conservation of mass, momentum, and energy fluxes across this layer leads to a relationship between the nonequilibrium thermodynamic properties at the surface and the equilibrium thermodynamic properties at the outer edge of the Knudsen layer. Total energy conservation gives a relationship between the incident radiation flux and the mass loss rate.

Received Jan. 29, 1990; revision received June 15, 1990; accepted for publication July 5, 1990.

*Scientist, Div. 104, 2860 S. Circle Dr., Suite 2340.
†Scientist, Div. 356, 2109 Air Park Road, SE.

Model Development

Single-Species Vaporization

The distribution of molecular velocities for molecules emitted from a vaporizing surface is assumed to be a half-range Maxwellian distribution function. Under saturation conditions, where the vapor pressure equals the equilibrium vapor pressure, the backscattered molecules returning to the surface have an equal half-range Maxwellian distribution, and the sum constitutes a gas in equilibrium. Under conditions of rapid vaporization there are many more molecules leaving the surface than there are molecules returning to it, and the gas is not in translational equilibrium at the vaporizing surface. An equilibrium distribution of molecular velocities develops by a collision process as the gas moves away from the surface. Thus, nonequilibrium dynamic conditions exist for a length of a few molecular mean free paths out from the surface. This region is the Knudsen layer. For modeling purposes we will assume that the molecular velocity distribution at the surface applies throughout the Knudsen layer and that there is an abrupt transition to the equilibrium Maxwellian distribution at the outer edge of the layer. (This assumption simplifies visualization, but is not critical; the actual solution presented depends only on conservation of mass, momentum, and energy across the Knudsen layer, and it does not matter whether the change in velocity is abrupt or smooth.) In the following discussion thermodynamic properties at the interface between the ablating surface and the nonequilibrium gas layer are designated by the subscript s, and thermodynamic properties at the boundary between the nonequilibrium and equilibrium layers are designated by the subscript e.

In Knight's treatment of rapid vaporization for a single species[2] the distribution of molecular velocities in the nonequilibrium region (at the s surface), f_s, is assumed to be half-Maxwellian combined with a backscattered term that is proportional to the Maxwellian distribution in the equilibrium region (at the e surface), f_e:

$$f_s = \begin{cases} \rho_s(M/2\pi RT_s)^{3/2} \exp\{-Mv^2/2RT_s\}, & v_x > 0 \\ \beta f_e, & v_x < 0 \end{cases} \tag{1}$$

$$f_e = \rho_e(M/2\pi RT_e)^{3/2} \exp\{-M(v-u)^2/2RT_e\} \tag{2}$$

where β is the backscattering coefficient, a dimensionless parameter; ρ_e is the gas density at the boundary of the equilibrium region; ρ_s is the gas density at the surface; M is the molecular mass; R is the universal gas constant; T_e and T_s are the gas temperatures at the equilibrium surface and at the vaporizing surface, respectively; v is the molecular velocity; u

is the mean efflux velocity in the equilibrium region (i.e., the net vapor flow away from the vaporizing solid); and $(v-u)^2 = (v_x-u)^2 + v_y^2 + v_z^2$. The x direction is taken as normal to the surface.

The fraction of molecules that return to the surface and recondense is given by the condensation coefficient α, and the mass flux across the Knudsen layer is

$$J_s = \int v_x f_s \, dV_+ + \int v_x f_s \, dV_- - (1-\alpha)\int v_x f_s \, dV_- \tag{3}$$

where the subscript plus denotes the velocity half-space $v_x > 0$, and the subscript minus denotes the velocity half-space $v_x < 0$. The Knudsen layer is taken to be of negligible thickness, and the integrals are evaluated over the full range of velocity space. The three terms on the right-hand side of Eq. (3) represent the vaporizing molecules leaving the surface, the backscattered molecules, and the molecules returning to the surface that do not recondense, respectively. The noncondensing molecules are assumed to reflect off the surface. The mass flux in the equilibrium region is

$$J_e = \int v_x f_e \, dV = \rho_e u \tag{4}$$

Similar expressions can be written for the momentum flux and energy flux. Conservation of mass, momentum, and energy across the Knudsen layer results in the following equations:

$$\int v_x f_e \, dV = \int v_x f_s \, dV_+ + \alpha\beta \int v_x f_e \, dV_- \tag{5}$$

$$\int v_x^2 f_e \, dV = \int v_x^2 f_s \, dV_+ + (2-\alpha)\beta \int v_x^2 f_e \, dV_- \tag{6}$$

$$\int (v^2/2 + \epsilon_e) v_x f_e \, dV = \int (v^2/2 + \epsilon_s) v_x f_s \, dV_+ + \alpha\beta \int (v^2/2 + \epsilon_e) v_x f_e \, dV_- \tag{7}$$

where ϵ is the energy per unit mass due to internal degrees of freedom, i.e., the specific internal energy u_{int} less the energy per unit mass due to translational degrees of freedom (with the subscript denoting the value of ϵ at T_e or T_s):

$$\epsilon = u_{\text{int}} - 3RT/2M = h - 5RT/2M \tag{8}$$

where h is the specific enthalpy. Assuming that the ratio of heat capacities γ is constant,

$$\epsilon = RT/[M(\gamma-1)] - 3RT/2M = RT(5-3\gamma)/(2M(\gamma-1)) \tag{9}$$

If the vaporizing material forms a single gaseous species, Eqs. (5–7) can be integrated to obtain a system of three equations:

$$\rho_e u = \rho_s (RT_s/2\pi M)^{1/2} + \alpha\beta\rho_e (RT_e/2\pi M)^{1/2} F_1(m) \tag{10}$$

$$\rho_e (u^2 + RT_e/M) = \rho_s (RT_s/2M) + (2-\alpha)\beta\rho_e (RT_e/M) F_2(m) \tag{11}$$

$$\rho_e u((5RT_e/2M) + u^2/2) = \rho_s (RT_s/2\pi M)^{1/2}(2RT_s/M + \epsilon_s - \epsilon_e) + \alpha\beta\rho_e (RT_e/2\pi M)^{1/2}(RT_e/M) F_3(m) \tag{12}$$

where

$$F_1(m) = (m\sqrt{\pi}) \operatorname{erfc}(m) - \exp(-m^2) \tag{13}$$

$$F_2(m) = (m^2 + 1/2) \operatorname{erfc}(m) - (m/\sqrt{\pi}) \exp(-m^2) \tag{14}$$

$$F_3(m) = 2F_1(m) + (m\sqrt{\pi}) F_2(m) \tag{15}$$

$$m = u(M/2RT_e)^{1/2} \tag{16}$$

and $\operatorname{erfc}(m)$ is the complementary error function.

For vaporization into a vacuum, u is set equal to the sonic velocity, which, for an ideal gas, is

$$u = (\gamma RT/M)^{1/2} \tag{17}$$

For expansion against backpressure m would be treated as a parameter determined by conditions outside the Knudsen layer, as in Ref. 2. The dimensionless parameter m in Eq. (16) then reduces to $(\gamma/2)^{1/2}$, and for unit condensation ($\alpha = 1$), Eqs. (10–12) reduce to Knight's results.

Using ϵ in the form of Eq. (9), Eqs. (10–12) with $\alpha = 1$ can be manipulated to yield closed expressions for (T_e/T_s), (ρ_e/ρ_s), and β as given by Knight[2]:

$$T_e/T_s = [(1+x^2)^{1/2} - x]^2 \tag{18}$$

where

$$x = (m\sqrt{\pi}/2)[(\gamma-1)/(\gamma+1)]$$

$$\rho_e/\rho_s = \tau[F_2(m) - \tau F_1(m)/2] \exp(m^2) \tag{19}$$

where

$$\tau = (T_s/T_e)^{1/2}$$

and

$$\beta = [(2m^2+1) - m\tau\sqrt{\pi}]\tau(\rho_s/\rho_e) \exp(m^2) \tag{20}$$

If the nonequilibrium vapor pressure at the surface, p_s, is assumed to be given by a Clausius-Clapeyron relationship,

$$p_s = p_0 \exp(-E_0/RT_s) \tag{21}$$

then the mass flux $J_e = \rho_e u$, given by Eq. (10), can be written in closed form as

$$J_e = \rho_s (RT_s/2\pi M)^{1/2}(1-B) = p_0 (M/2\pi RT_s)^{1/2}(1-B) \exp(-E_0/RT_s) \tag{22}$$

where B is the fraction of the initial vaporization flux that is backscattered and recondenses on the surface (backscattering fraction). B is given by

$$B = -\beta(\rho_e/\rho_s)(T_e/T_s)^{1/2} F_1(m) \tag{23}$$

The quantities T_e/T_s, ρ_e/ρ_s, β, and B and the ratio of pressures p_e/p_s depend only on the ratio of heat capacities, γ. These values are listed in Table 1 for various values of γ. [Values for γ correspond to monatomic (5/3), diatomic (7/5), and polyatomic (4/3) ideal gases without vibrational degrees

Table 1 Dependence of T_e/T_s, ρ_e/ρ_s, β, B, and p_e/p_s on γ

γ	T_e/T_s	ρ_e/ρ_s	β	B	p_e/p_s
1.667	0.669	0.308	6.287	0.184	0.206
1.400	0.782	0.301	5.475	0.212	0.235
1.333	0.814	0.299	5.260	0.219	0.243
1.286	0.837	0.298	5.105	0.224	0.250
1.167	0.901	0.297	4.712	0.237	0.267
1.000	1	0.296	4.154	0.257	0.296

Table 2 Carbon vapor parameters in the single species approximation

T_s, K	$<\gamma_s>$	T_e/T_s	$<\rho_e>/<\rho_s>$	β	B	J_e, kg/m²/s
3000	1.176	0.896	0.297	4.75	0.237	0.0216
4000	1.128	0.923	0.296	4.59	0.242	54.7
5000	1.090	0.947	0.296	4.45	0.246	5590
6000	1.090	0.946	0.296	4.46	0.246	25,600

of freedom, to a diatomic ideal gas with two vibrational degrees of freedom (9/7), and to intermediate (7/6) and limiting (1) values.]

Examination of the B column shows that, under conditions of rapid vaporization into a vacuum, 18–25% of the emitted vaporization flux is backscattered to the surface.

A reasonable estimate of the carbon mass flux for vaporizing graphite can be obtained by using a single effective species approximation, where the carbon molecules of the different molecular species are assumed to have a mean molecular mass $<M_s>$ given by

$$<M_s> = <\rho_s>/\Sigma(\rho_{si}/M_i) \tag{24}$$

and a mean value of $<\gamma_s>$ satisfying

$$[<\rho_s>/<M_s>(<\gamma_s> - 1)] = \Sigma[\rho_{si}/M_i(\gamma_i - 1)] \tag{25}$$

where the properties of the various species are denoted by the subscript i.

The various dimensionless parameters and the carbon mass flux at different temperatures were calculated using theoretical thermodynamic properties for seven carbon species, C_1–C_7, presented by Leider et al.[5] and by Lee and Sanborn.[6] The results are summarized in Table 2.

The quantities T_e/T_s, $<\rho_e>/<\rho_s>$, β, and B exhibit a temperature dependence because the data of Leider et al.[5] have different activation energies for the vaporization partial pressures of the various carbon species. Consequently, the mole fractions of the different species and therefore the value of $<\gamma_s>$ show a temperature dependence. (It should be noted that the values for γ_i inferred from Lee and Sanborn[6] imply a slight temperature dependence. The calculations summarized in Table 2 were made under the assumption that the mean value of γ is constant over the temperature range of T_s to T_e. When the temperature dependence of the mean value of γ is taken into account, calculations show very little difference from the results in Table 2.)

The dominant temperature dependence of the vaporization mass flux J_e was found to result from the temperature dependence of the vaporization pressure of carbon. Consequently, the vaporization mass flux is well approximated by an Arrhenius form,

$$J_e = A \exp(-E_0/RT_s) \tag{26}$$

[The pre-exponential term in Eq. (22) is only weakly dependent on temperature.] There is a change in properties at the theoretical melting temperature, 4765 K. A two-piece, least-squared fit to the data gives values for A and E_0 listed in Table 3 for a transition at 4765 K.

Table 3 Two-piece fit of Eq. (26) for the single carbon species model

	Below 4765 K	Above 4765
A	1.93×10^{12} kg/m²/s	4.68×10^{7} kg/m²/s
E_0	804,000 J/mole	375,500 J/mole

Table 4 Mean number carbon atoms per molecule and mean molecular mass of carbon vapor as a function of surface temperature

T_s, K	No.	$<M_s>$, kg/mole	T_s, K	No.	$<M_s>$, kg/mole
3000	2.755	0.03309	4765	4.176	0.05016
3200	2.807	0.03371	4800	4.175	0.05015
3400	2.862	0.03438	5000	4.165	0.05003
3600	2.928	0.03517	5500	4.112	0.04951
3800	3.015	0.03621	6000	4.051	0.04866
4000	3.138	0.03769	6500	3.970	0.04768
4200	3.314	0.03980	7000	3.891	0.04673
4400	3.558	0.04274			
4600	3.872	0.04651			

Table 5 Carbon vapor parameters for the seven carbon species approximations, $\epsilon = h(T) - 2.5(RT/M)$

T_s, K	T_e/T_s	$<\rho_e>/<\rho_s>$	β	B	J_e, kg/m²/s
3000	0.892	0.297	4.53	0.226	0.0217
4000	0.919	0.294	4.41	0.233	54.7
5000	0.945	0.292	4.10	0.232	5570
6000	0.943	0.291	4.04	0.228	25,500

Multiple-Species Treatment

For graphite the carbon gas is assumed to comprise n molecular species. Baker[3] and Risch and Kelly[4] assume that molecular velocity distributions of the form in Eqs. (1) and (2) hold for each molecular species. For simplicity it is assumed that the molecular species do not interact chemically once they leave the vaporizing surface and that all backscattered molecules recondense upon return to the surface. (Performing the solution for the case in which the different carbon species are allowed to interact produces only minor differences in the results.) Conservation of mass flux holds for each molecular species, yielding n equations in the form of Eq. (10):

$$\rho_{ei}u = \rho_{si}(RT_s/2\pi M_i)^{1/2} + \beta\rho_{ei}(RT_e/2\pi M_i)^{1/2}F_1(m_i) \tag{27}$$

Conservation of the total momentum flux and the total energy flux yield two additional equations:

$$<\rho_e>(u^2 + RT_e/<M_e>) = <\rho_s>(RT_s/2<M_s>) + \beta RT_e\Sigma(\rho_{ei}/M_i)F_2(m_i) \tag{28}$$

$$<\rho_e>u[u^2/2 + (5RT_e/2<M_e>)] = (RT_s/2\pi)^{1/2}\Sigma(\rho_{si}/\sqrt{M_i})(2RT_s/M_i + \epsilon_{si} - \epsilon_{ei}) + \beta[(RT_e)^3/2\pi]^{1/2}\Sigma(\rho_{ei}/M_i^{3/2})F_3(m_i) \tag{29}$$

where $<\rho_e> = \Sigma\rho_{ei}$, $<\rho_s> = \Sigma\rho_{si}$; $<M_e>$ and $<\gamma_e>$ are analogous to $<M_s>$ and $<\gamma_s>$ in Eqs. (24) and (25); and m_i is the value of m as in Eq. (16) for species i, with the sonic velocity taken as

$$u = (<\gamma_e>RT_e/<M_e>)^{1/2} \tag{30}$$

The mean molecular mass of the carbon gases as a function of surface temperature, computed from the data of Ref. 5, is given in Table 4.

The system of Eqs. (27–29) is solved iteratively to obtain numerical values for T_e/T_s, $<\rho_e>/<\rho_s>$, and β. The mass flux is the sum of Eq. (27) over i and can be written as

$$J_e = (RT_s/2\pi)^{1/2}\Sigma(\rho_{si}/\sqrt{M_i})(1 - B_0) \tag{31}$$

where B_0 is the fraction of the vaporization flux that returns to the surface:

$$B_0 = \frac{-\beta(T_e/T_s)^{1/2}\Sigma(\rho_{ei}F_1(m_i)/\sqrt{M_i})}{\Sigma(\rho_{si}/\sqrt{M_i})} \tag{32}$$

The various dimensionless parameters and the carbon mass flux at different temperatures were calculated using theoretical thermodynamic properties from Leider et al.[5] and Lee and Sanborn.[6] The results are summarized in Table 5.

In the preceding results an expression of the form given in Eq. (8) was used for the energy due to internal degrees of freedom. [Using the form given in Eq. (9) gave only minor differences.] A comparison of Tables 5 and 2 reveals some differences, but the carbon mass flux is nearly identical.

Least-squares fits of the data to Eq. (26) give values for A and E_0 listed in Table 6. The curves cross at 4850 K due to the fit.

Modification due to Pyrolytic Gas

The thermal decomposition of organic resins occurs at temperatures much lower than those required for significant carbon vaporization. Heating the surface of a composite material such as graphite-epoxy with incident energy will act to pyrolyze the surface resin and leave behind graphitic char and the graphite fibers themselves. As the irradiation continues, the surface temperature will rise, and resin below the surface will become hot enough to pyrolyze. The gases liberated during pyrolysis escape through the porous char and become hotter as they approach the surface. Various chemical reactions may occur between the gases and the solid carbon (particularly thermal cracking and deposition of additional carbon) during this process, but this is not of concern to the present discussion. The significant feature is that the hot, graphitized surface will generally be at a far higher temperature than the equilibrium vaporization temperature of the gases diffusing outward from the interior of the material as a result of pyrolysis. Unlike carbon vapor species, the molecules of these gases will not condense on the surface. It is reasonable, therefore, to set the condensation coefficient for the pyrolytic gases equal to zero. For the pyrolytic gases, $\alpha = 0$, and Eqs. (10–12) reduce to

$$\rho_e u = \rho_s(RT_s/2\pi M)^{1/2} \tag{33}$$

$$\rho_e(u^2 + RT_e/M) = \rho_s(RT_s/2M) + 2\beta\rho_e(RT_e/M)F_2(m) \tag{34}$$

$$\rho_e u[u^2/2 + (5RT_e/2M)] = \rho_s(RT_s/2\pi M)^{1/2}(2RT_s/M + \epsilon_s - \epsilon_e) \tag{35}$$

The gas flux, and hence the gas density at the surface, are determined by the pyrolysis reaction rate below the surface. It is assumed that the escape of the pyrolytic gas through the porous graphite is sufficiently slow to allow the gas to attain a temperature T_s at the surface.

A mixture of carbon vapor and pyrolytic gases will emanate from the surface. The presence of volatile gases mixed with the carbon vapors alters the gasdynamics and modifies the carbon vapor flux. To illustrate the effect of the pyrolytic gas, consider Eqs. (27–29), augmented by a single, noncondensing gas with properties designated by the subscript p. (The pyrolysis gas actually includes a variety of molecular species, but its effect on the gasdynamics can be approximated by a single species with mean properties.) The conservation equations for chemically noninteracting gases then become

$$\rho_{ep}u = \rho_{sp}(RT_s/2\pi M_p)^{1/2} \tag{36}$$

$$\rho_{ei}u = \rho_{si}(RT_s/2\pi M_i)^{1/2} + \beta\rho_{ei}(RT_e/2\pi M_i)^{1/2}F_1(m_i) \tag{37}$$

$$<\rho_e>(u^2 + RT_e/<M_e>) = <\rho_s>(RT_s/2<M_s>) \beta RT_e[2(\rho_{ep}/M_p)F_2(m_p) + \Sigma(\rho_{ei}/M_i)F_2(m_i)] \tag{38}$$

$$<\rho_e>u[u^2/2 + (5RT_e/2<M_e>)] = (RT_s/2\pi)^{1/2}[\Sigma(\rho_{si}/\sqrt{M_i})(2RT_s/M_i + \epsilon_{si} - \epsilon_{ei}) + (\rho_{sp}/\sqrt{M_p})(2RT_s/M_p + \epsilon_{sp} - \epsilon_{ep})] + \beta[(RT_e)^3/2\mathrm{P}]^{1/2}\Sigma(\rho_{ei}/M_i^{3/2})F_3(m_i) \tag{39}$$

The model can be extended to include multiple pyrolytic species, but the present analysis will be limited to one. The mean molecular mass of the escaping gases is then

$$<M_e> = (J_c + J_p)/[(J_c/<M_c>) + (J_p/M_p)] \tag{40}$$

where $J_c = <\rho_{ec}>u$ is the carbon mass flux; $J_p = <\rho_p>u$ is the pyrolysis gas mass flux; M_c and M_p are the mean molecular

Table 6 Least-squares fit parameters to Eq. (26) for the seven carbon species model

	Below 4765 K	Above 4765 K
A	1.90×10^{12} kg/m^2/s	4.90×10^7 kg/m^2/s
E_0	804,000 J/mole	377,500 J/mole

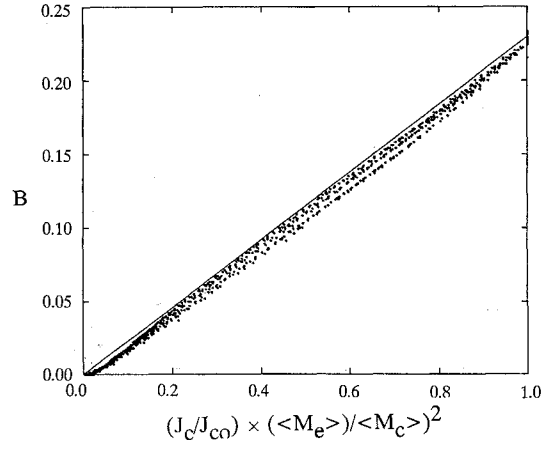

Fig. 1 Backscattering fraction for different pyrolytic outgassing conditions.

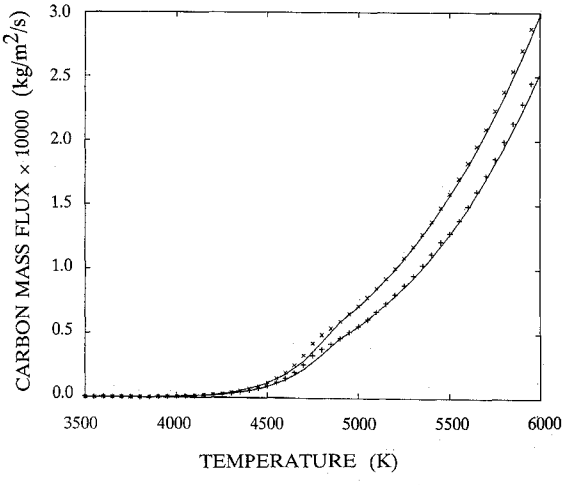

Fig. 2 Comparison of the simplified model to the detailed model.

masses of the carbon gases and pyrolysis gases, respectively, as in Eq. (24); and m_i and m_p are analogous to m in Eq. (16). [It is assumed that the sonic velocity can be written as in Eq. (30) with $<\gamma_e>$ calculated as in Eq. (25), except that the summation over i includes the pyrolysis gases as well as the carbon species.]

Equations (36–39) can be solved iteratively for T_e/T_s, $<\rho_e>/<\rho_s>$, and β, and the mass loss rate can be calculated using the partial pressures for carbon vaporization and the pyrolytic gas flux.

The carbon mass flux is the sum of Eq. (37) over i and can be written as

$$J_c = (RT_s/2\pi)^{1/2}\Sigma(\rho_{si}/\sqrt{M_i})(1-B) \tag{41}$$

where B is the carbon backscattering fraction:

$$B = \frac{-\beta(T_e/T_s)^{1/2}\Sigma[\rho_{ei}F_1(m_i)/\sqrt{M_i}]}{\Sigma(\rho_{si}/\sqrt{M_i})} \tag{42}$$

The effect of the pyrolytic gas is to modify the sonic velocity of the escaping mixed gases. In the case of a decomposing organic resin the presence of hydrogen produces a smaller mean molecular mass $<M_e>$ for the gas mixture than for the carbon gases alone, resulting in an increased sonic velocity [Eq. (17)]. As the carbon molecules move across the Knudsen layer, they encounter a lighter, more rapidly moving gas in the equilibrium region. Consequently, a smaller fraction of the carbon vaporization flux is backscattered, and the carbon mass flux for a given surface temperature is increased. In the limiting case where the pyrolytic gas flux is much larger than the carbon vaporization flux and where the pyrolytic gas is assumed to be pure hydrogen, the value of B is nearly zero. For (hypothetical) pyrolytic gases more massive than the carbon gas, the model predicts a reduced carbon mass flux.

Simplified Model

The quantities β, T_e/T_s, ρ_{ei}, and m_i in Eq. (42) are modified by the pyrolytic gas flux, which is controlled by phenomena apart from the surface temperature. To determine B, an iterative solution to Eqs. (36–39) is required for a given pyrolytic gas flux and surface temperature. By varying the pyrolytic gas flux $J_{ep} = \rho_{ep}u$ and the mean molecular mass $<M_p>$, B was found to be well approximated by

$$B = (J_c/J_{co})(<M_e>/<M_c>)^2 B_0 \tag{43}$$

where $J_c = <\rho_{ec}>u$ is the modified carbon mass flux, $J_{co} = <\rho_{eco}>u_0$ is the unmodified carbon mass flux (zero pyrolytic gas flux) given by Eq. (26) using the parameters in Table 6, and B_0 is the value of B for zero pyrolytic gas flux. From Table 5 it is apparent that B_0 is nearly independent of temperature. Figure 1 is a plot of the backscattering fraction B vs the dimensionless parameter $(J_c/J_{co})(<M_e>/<M_c>)^2$ for various conditions (different pyrolysis gas fluxes, different molecular masses, and different surface temperatures). The straight line is a plot of Eq. (43) with $B_0 = 0.23$.

The factor

$$(RT_s/2\pi)^{1/2}\Sigma(\rho_{si}/\sqrt{M_i})$$

in Eq. (41) is independent of pyrolytic gas flux and can be rewritten in terms of the unmodified carbon mass flux and backscattering fraction. Equation (41) then becomes

$$J_c = J_{co}(1-B)/(1-B_0) \tag{44}$$

The modified carbon flux is calculated using the following iterative scheme:

1) Obtain an initial estimte of J_c using Eq. (26).
2) Calculate $<M_e>$ using Eq. (40).
3) Calculate B using Eq. (43).
4) Calculate J_c using Eq. (44).
5) Repeat steps 2–4 until J_c converges.

The values of $<M_c>$ are given as $<M_s>$ in Table 4.

In Fig. 2 the carbon mass flux given by this simplified model (solid curves) is compared to the carbon mass flux calculated using the multiple-species method (points) described in the model development section. The comparison is made for vaporization of pure graphite (+) and for graphitic char with a nominal pyrolysis outgassing of 1000 kg/m^2/s of H_2 (×).

Finally, it is interesting to note the results of computer simulations of ablation of graphite-epoxy. A comparison was made between a model that assumed the carbon vaporization rate of graphite and one where the modification described earlier was taken into account. The increased carbon mass flux predicted by the latter model transports more energy away from the surface, and requirements of energy balance force a lower surface temperature. The result is that, for a given incident energy flux, the carbon mass loss rate for both models is nearly identical. The implication is that energy conservation gives the proper mass flux irrespective of which physical model is used; however, consideration of the modification due to pyrolytic outgassing may be important in considering thermal effects.

Conclusions

The presence of noncondensable gases from the pyrolysis of organic materials influences the carbon mass loss rate for vaporizing graphite. The mass loss calculated from the consideration of the gasdynamics of multiple gas species is well approximated by a simple algorithm that relates B to the modified carbon mass flux.

References

[1]Anisimov, S., "Vaporization of Metal Absorbing Laser Radiation," *Soviet Physics JETP*, Vol. 27, July 1968, pp. 182, 183.

[2]Knight, C. J., "Theoretical Modeling of Rapid Surface Vaporization with Back Pressure," *AIAA Journal,* Vol. 17, May 1979, pp. 519–523.

[3]Baker, R. L., "Carbon Nonequilibrium Phase Change," Aerospace Corp., El Segundo, CA, Interim Rept. SD-TR-81-89, 1981.

[4]Risch, T. K., and Kelly, J. T., "A Model for Radiation Driven Ablation of Carbon Under Low Pressures," *Society of Automotive Engineers,* Paper 851396, Fifteenth Intersociety Conference on Environmental Systems, San Francisco, CA, July 15–17, 1985.

[5]Leider, H. R., Krikorian, O. H., and Young, D. A., "Thermodynamic Properties of Carbon up to the Critical Point," *Carbon,* Vol. 11, Pergamon, London, 1973, pp. 555–563.

[6]Lee, E. L., and Sanborn, R. H., "Extended and Improved Thermal Functions for the Gaseous Carbon Species C_1–C_7 from 298 to 10,000 K," *High Temperature Science,* Vol. 5, Academic, London, 1973, pp. 438–453.